Thermokinetic Proton Transfer and Ab Initio Studies of the $[2H,S,O]^+$ System. The Proton Affinity of HSO

Brian K. Decker,[†,§] Nigel G. Adams,[*,†] Lucia M. Babcock,[†] T. Daniel Crawford,[‡,||] and Henry F. Schaefer, III[‡]

Department of Chemistry, The University of Georgia, Athens, Georgia 30602, and Center for Computational Quantum Chemistry, The University of Georgia, Athens, Georgia 30602

Received: February 24, 2000

The $[2H,S,O]^+$ ionic system has been studied jointly with a selected ion flow tube (SIFT) and by coupled cluster ab initio methods. Experimentally, the $[2H,S,O]^+$ ions were generated by the reaction of $SO^+(X\ ^2\Pi_r)$ with C_2H_6, and reacted at room temperature with CH_3SH, *n*-C_3H_6, HCO_2H, *o*-$C_6H_4F_2$, $CF_3C(O)CH_3$, CH_2O, H_2S, c-C_6H_{12}, CS_2, C_2H_4, and SO_2 comprising a series of reference bases with gas basicities ranging from 177 to 154 kcal mol^{-1}. Thermokinetic analysis of the proton-transfer efficiencies in these reactions yields a free energy of proton detachment of 163.6 ± 2.2 kcal mol^{-1} for $HSOH^+$. The results of the ab initio study are used to determine the relationship of this proton detachment energy to the various isomeric forms of $[2H,S,O]^+$ and the two isomers HSO and SOH. The resulting best values for the gas-phase basicity and the proton affinity of HSO at 298 K are 163.6 (+4.6, −2.2) kcal mol^{-1} and 171.0 (+4.6, −2.4) kcal mol^{-1}, respectively. Observation of the charge-transfer behavior of $HSOH^+$ with the selected neutral bases restricts the recombination energy of $HSOH^+$ to the range 9.5 ± 0.2 eV. Rate coefficients and product distributions for the reactions of $HSOH^+$ with the bases in the bracketing study are presented and discussed, as well as the results of the ab initio study and the interpretation of the thermokinetic data. Additionally, a revised determination of the gas-phase basicity, proton affinity, and enthalpy of formation of HS_2 at 298 K (from the proton-transfer reactions of $HSSH^+$) is presented, which increases those quantities by 0.8 kcal mol^{-1} to 170.6 ± 2.2, 178.8 ± 2.4, and 25.8 ± 2.5 kcal mol^{-1}, respectively.

1. Introduction

The thioperoxy radical, HSO, has been a subject of numerous experimental[1] and theoretical[2] studies due to its potential importance as a reactive intermediate in the chemistry of atmospheric sulfur.[3] A number of determinations of the absolute and relative thermodynamic stabilities of HSO and its structural isomer, SOH, have been made,[1a−e,2] most of which have been tabulated by Goumri et al.[2a] In a high-level ab initio study of HSO and SOH, using a complete active space self-consistent field (CASSCF)/second-order configuration interaction (SOCI) methodology with a large cc-pV5Z basis set, Xantheas and Dunning[2f] computed upper-limit enthalpies of formation at 298 K ($\Delta H_f°_{298}$) of −6.1 ± 1.3 and −0.7 ± 1.3 kcal mol^{-1}, respectively. Accurate thermochemical data for HSO and SOH are necessary to determine their roles in the recycling of reduced forms of sulfur and destruction of ozone in the stratosphere through reactions such as

$$HSO + O_3 \rightarrow HS + 2O_2 \qquad (1)$$

Because of the similar enthalpies of formation of ozone and the mercapto radical, the exothermicity of this reaction is critically dependent upon the enthalpy of formation of HSO.

Although detection of neither HSO nor SOH in interstellar clouds (ISC) has yet been reported, we have shown very recently that these are likely to be important interstellar species.[4] The reactions of SO^+, an abundant and nearly ubiquitous interstellar ion,[5] with many organic molecules detected in ISC have been shown experimentally to lead to the formation of HSO and/or SOH.[4a,c] Reactions of atomic S^+ with organic molecules containing oxygen frequently also form these radical species.[4b,c] Thermochemical data, such as the proton affinities of HSO and SOH, are important for determining the dominant forms of these radicals in ISC and, consequently, which reactive processes (e.g., electron/ion dissociative recombination, ion/molecule reactions, neutral/neutral reactions, photodissociation, etc.) are likely to be important for their creation and destruction. The microwave spectra of HSO and its isotopomer DSO have been recorded,[1u] and both HSO[1t] and SOH (see Supporting Information) have quite substantial electric dipole moments, and thus should be highly detectable. Searches for new interstellar molecules should include these species.

Protonated HSO/SOH may be considered as singly ionized forms of the [2H,S,O] family of molecules, which includes H_2-SO (dihydrogen sulfoxide), HSOH (hydrogen thioperoxide), and H_2OS (dihydrogen thiooxonium ylide). Several ab initio studies have considered neutral HSOH;[6] fewer have focused on H_2SO[6c−e] or H_2OS.[6c] Wolfe and Schlegel[6c] have made the only study comparing the energetics of all three isomers, in which they found H_2SO and H_2OS to be ∼28 and ∼34 kcal mol^{-1} higher in energy than HSOH, respectively, at the MP4/6-31G-

* To whom all correspondence should be addressed. Fax: (706) 542-9454. E-mail: adams@sunchem.chem.uga.edu.

† Department of Chemistry, The University of Georgia.

‡ Center for Computational Quantum Chemistry, The University of Georgia.

§ Present address: Chemistry Division, Bldg. 200, Argonne National Laboratory, 9700 S. Cass Ave., Argonne, IL 60439. Fax: (630) 252-9292. E-mail: decker@anchim.chm.anl.gov.

|| Present address: Institute for Theoretical Chemistry, Departments of Chemistry and Biochemistry, The University of Texas, Austin, TX 78712-1167. Fax: (512) 471-8696. E-mail: crawdad@jfs1.cm.utexas.edu.

10.1021/jp000742e CCC: $19.00
Published on Web 04/26/2000

(d,p) level of theory. Isomerization barriers from these higher-energy isomers to HSOH were computed to be substantial, i.e., ~36 kcal mol^{-1} for H_2SO and ~12 kcal mol^{-1} for H_2OS.[6c] No computational studies have been published previously for the singly ionized $[2H,S,O]^+$ system; however, it is isoelectronic with the dihydrophosphoryl radical, H_2PO, which has been investigated recently at comparable levels of ab initio theory to those used here.[7]

Experimental observations of the [2H,S,O] and $[2H,S,O]^+$ systems of molecules are exceedingly sparse. Detection of hydrogen thioperoxide, HSOH, was first reported in 1977 by Smardzewski and Lin from the infrared absorption spectrum of an argon matrix containing O_3 and H_2S.[8] Indirect evidence for the gas-phase synthesis of HSOH was obtained from a thermochemical bracketing study of the HOS^- anion by O'Hair et al.,[1b] in which proton transfer to HOS^- from a series of reference acids, HA, was inferred from the detection of A^- in a tandem flowing afterglow-selected ion flow tube (FA-SIFT). More direct evidence for the existence of gas-phase HSOH and of its structural isomer, H_2OS, was obtained by Iraqi and Schwarz[9] from collisonal activation (CA) and neutralization−reionization (NR) experiments on the $[2H,S,O]^+$ ions generated in a chemiionization (CI) source coupled to a four-sector tandem mass spectrometer. In their CI source, Iraqi and Schwarz used a mixture of H_2S and N_2O to generate $HSOH^+$ and a mixture of CS_2 and H_2O to generate H_2OS^+; the specific chemical pathways leading to these ions were not discussed. Recently, in two SIFT studies, $[2H,S,O]^+$ was observed as a product in the ion/molecule reactions of[4a] $SO^+(X\ ^2\Pi_r)$ and[4b] $S^+(^4S)$ with several small organic molecules.

In the present work, we have employed experimental and computational methodologies to obtain previously unavailable thermochemical data for the $[2H,S,O]^+$ system of radical cations, and for the neutral radicals HSO and SOH derived therefrom. The $[2H,S,O]^+$ ions were synthesized in a SIFT by the reaction sequence[4a]

$$S^+(^4S) + O_2(X\ ^3\Sigma_g^-) \rightarrow SO^+(X\ ^2\Pi_r) + O(^3P) \qquad (2)$$

$$SO^+(X\ ^2\Pi_r) + C_2H_6 \rightarrow [2H,S,O]^+ + C_2H_4\ (80\%) \qquad (3)$$

$$\rightarrow C_2H_5^+ + HSO/SOH\ (20\%)$$

The bimolecular rate coefficients for reactions 2 and 3 are[10] $k_2^{(2)} = 1.8 \times 10^{-11}$ and[4a] $k_3^{(2)} = 1.3 \times 10^{-9}$ cm^3 $molecule^{-1}$ s^{-1}, respectively, at 298 K. Reaction 2 is exothermic by only 6.9 kcal mol^{-1} (using data available in ref 11), and thus can only populate the $v \leq 1$ vibrational levels of the ground $^2\Pi_r$ electronic state of SO^+.[12] The "end point" of reaction 2 (semiarbitrarily defined here as the point at which the precursor S^+ has declined to e^{-5}, or ~1%, of its initial concentration) occurred ~36 cm upstream from the addition point for C_2H_6 in our flow tube. In this region, approximately 80 collisions with O_2 and 2×10^4 collisions with He were experienced by each SO^+ molecule, removing vibrational excitation via V−V and V−T collisional de-excitation.[13] Since the experiments were performed in He carrier gas at a laboratory temperature of 294.5 ± 2.5 K, virtually no excess energy above the reaction exothermicity was available to drive reaction 3. As will be seen below, this exothermicity limited the possible isomeric forms of $[2H,S,O]^+$ which could be created.

The ion products of reaction 3 were reacted with the following series of reference bases, whose gas-phase basicities[14] in kcal mol^{-1} are given in parentheses: CH_3SH (177), *n*-C_3H_6 (172.7), HCO_2H (169.8), *o*-c-$C_6H_4F_2$ (168.1), $CF_3C(O)CH_3$ (165.4), CH_2O (163.3), H_2S (161.0), c-C_6H_{12} (159.4), CS_2 (157.2), C_2H_4 (155.7), SO_2 (153.8). Reaction rate coefficients and product distributions were determined and then interpreted using the thermokinetic method of Bouchoux et al.[15] The results are compared with a refitting of the Bouchoux thermokinetic equation to data from our previous study, in which we determined the gas-phase basicity of HS_2 from proton-transfer reactions of $HSSH^+$.[16] To complement and supplement the experimental results, the stable isomers of both the [2H,S,O] and the $[2H,S,O]^+$ systems, as well as HSO and SOH, were investigated at high levels of theory, up to cc-pV5Z/CCSD(T). Our experimental results and thermochemical data computed in our ab initio study are compared in order to identify the isomeric form of the $[2H,S,O]^+$ ions generated by reaction 3, as well as to improve the interpretation of our thermokinetic bracketing data.

2. Experimental Section

The experimental measurements in the present work were made with a SIFT, which has been described in detail previously.[17] Briefly, numerous ions (i.e., C^+, S^+, CS_2^{2+}, CS^+, S_2^+ and CS_2^+) were generated from CS_2 in a low-pressure electron impact ion source and focused into a quadrupole mass filter (QMF) by a series of electrostatic lenses. The QMF was tuned to select S^+ ions, which were then focused onto a 1.0 mm diameter hole in a molybdenum disk electrode separating the differentially pumped region of the low-pressure (~10^{-4} Torr) QMF housing from the higher-pressure (~0.5 Torr) flow tube. High-purity helium carrier gas (BOC, 99.997%), which had been further purified by passage through a liquid nitrogen-cooled molecular sieve trap, was introduced immediately after the disk electrode via a ring-shaped venturi inlet. The injected swarm of ions traveled in the helium with a group velocity of ~120 m s^{-1} and a center-of-mass kinetic temperature in equilibrium with the helium bath gas at 294.5 ± 2.5 K.

The injected S^+ precursor ions were reacted with gases and vapors introduced at various inlets available along the flow tube. Gaseous reagents were used without further purification, and liquid reagents were further purified by several freeze−pump−thaw cycles before use. Reagents were obtained from commercial sources with the following purities: CH_3SH (99.5+ %); *n*-C_3H_6 (99+ mol %); HCO_2H (99.4 wt %); *o*-c-$C_6H_4F_2$ (99.7 wt %); $CF_3C(O)CH_3$ (99.9 wt %); CH_2O (paraformaldehyde, 95 wt %); H_2S (99.5+ %); c-C_6H_{12} (98+ wt %); CS_2 (99.99 wt %); C_2H_4 (99.5 mol %); SO_2 (99.98+ mol %); C_2H_6 (99.0+ mol %); O_2 (99.98+ mol %). Reagent throughputs were determined using calibrated capillary tubes operating under Poiseuille flow conditions. The gas-phase viscosities necessary for these determinations were taken from the literature[18] where possible; otherwise, they were determined experimentally from the pressure drop in a calibrated volume filled with the reagent vapor as it escaped to a vacuum through a calibrated capillary tube. Permanent gases and liquid vapors were introduced neat into the flow line, except for HCO_2H, which was introduced from a dilute (2.5%) manometric mixture in pure helium. Corrections for the monomer/dimer equilibrium shift of HCO_2H upon dilution were made using the data of Taylor and Bruton.[19] Formaldehyde was introduced neat into the flow line as it evolved from solid paraformaldehyde maintained at ~110 °C.

Reactant and product ions were sampled downstream through a 0.3 mm diameter hole in a molybdenum disk electrode separating a second differentially pumped housing (at ~10^{-5} Torr) containing a scannable quadrupole mass spectrometer

(QMS) (Extrel C-60) and a channel electron multiplier (Detech). Ion signals were amplified, passed to a pulse counter (Stanford Research Systems SR-400), and thence to a desktop computer for data storage and processing. Reaction rate coefficients and product distributions were determined in the usual way.[20] Rate coefficients are estimated to be accurate to ±20% for the permanent gases and ±30% for the vapors, the HCO_2H mixture in helium, and the CH_2O from paraformaldehyde. Reproducibility of the rate coefficients is ±10% or better. Fractional product distributions are considered to be accurate to ±0.05. Mass discrimination in the detection system was corrected, where necessary, as described previously.[16]

3. Computational Methods

The molecular properties of the $[2H,S,O]^+$ isomers were computed using coupled cluster (CC) methods,[21] including the singles and doubles (CCSD) model[22] and CCSD augmented with a perturbative estimate of the effects of connected triple excitations [CCSD(T)].[23] All coupled cluster computations were based on spin-unrestricted Hartree−Fock (UHF) reference determinants. The Dunning correlation-consistent polarized valence double-ζ (cc-pVDZ), triple-ζ (cc-pVTZ), quadruple-ζ (cc-pVQZ), and quintuple zeta (cc-pV5Z) basis sets were used,[24] as well as the core-correlation and weighted-core-correlation counterparts[25] of the double-ζ (cc-pCVDZ and cc-pwCVDZ) and triple-ζ (cc-pCVTZ and cc-pwCVTZ) basis sets. Geometries of all isomers were optimized using coupled cluster analytic gradient methods[26] and the cc-pVDZ and cc-pVTZ basis sets. An energy optimum structure was assumed to have been obtained once the root-mean-square of the internal coordinate forces fell below a threshold of 1.0×10^{-5} E_h/a_0. Harmonic vibrational frequencies were computed using finite differences of analytic energy gradients computed at geometries displaced from the corresponding stationary point. In geometry optimizations and frequency analyses, all electrons were correlated; for single-point energies, all electrons were correlated when using the cc-pCVXZ and cc-pwCVXZ basis sets, while only the valence electrons were correlated with the cc-pVXZ basis sets. All coupled cluster computations were carried out using the ACESII package of quantum chemical programs.[27]

The heats of formation of the $[2H,S,O]^+$ isomers were determined using two different reference reactions:

SCHEME 1

$$[2H,S,O]^+ \rightarrow SO^+ + H_2$$

SCHEME 2

$$2[2H,S,O]^+ \rightarrow H_2S^+ + SO^+ + H_2O$$

Scheme 1 is appropriate for such computations because it is isogyric and requires only the experimental values for $\Delta H_f^\circ{}_{298}$(SO) and the ionization potential (IP) of SO. Scheme 2 is both isogyric and isodesmic, and is expected to reduce differential correlation errors due to bonding pattern differences. In addition to the experimental values for $\Delta H_f^\circ{}_{298}$(SO) and IP(SO), Scheme 2 also requires $\Delta H_f^\circ{}_{298}(H_2S)$, $\Delta H_f^\circ{}_{298}(H_2O)$, and IP($H_2S$). All experimental thermochemical data were taken from the 1998 JANAF tables;[28] the experimental IP's of SO and H_2S were taken from refs 29 and 30, respectively (see Table 1).

Reaction energies for all species in Schemes 1 and 2 as well as the four $[2H,S,O]^+$ isomers of Tables 4−7 and the neutral [2H,S,O] and [H,S,O] isomers in Tables 1S−5S of the Supporting Information were determined from absolute energies computed using three methods: (1) all-electron cc-pVTZ/CCSD(T) energies computed at geometries optimized at that same level of theory for all species; (2) energies obtained using the Gaussian-2 (G2) method;[31,32] and (3) coupled cluster energies adjusted to the complete basis set (CBS) limit and for higher correlation effects using an extrapolation scheme similar to that described by King and co-workers.[33] Method (3) is based on the following procedure: Using cc-pVTZ/CCSD(T) optimized geometries, UHF energies were extrapolated to the basis-set limit using a three-parameter exponential function of the form[24a,34]

$$E_X = E_\infty + Ae^{-BX} \quad (4)$$

where X represents the cardinal number of the cc-pVXZ basis set (e.g., for cc-pVDZ, $X = 2$). The CCSD and CCSD(T) correlation energies were each fit to a two-parameter function of the form[35]

$$E_X = E_\infty + A/X^3 \quad (5)$$

In both cases, only energies computed using the cc-pVTZ, cc-pVQZ, and cc-pV5Z basis sets were used for the extrapolations and a separate fit was used for each molecular species. As a measure of the validity of the above extrapolation scheme, a mixed exponential/Gaussian function of the form recommended by Peterson et al.[36] was applied to obtain CBS energies for comparison to those computed using eqs 4 and 5. For relative energies of the four isomers of $[2H,S,O]^+$, the two schemes differed by at most 0.4 kcal mol^{-1}, suggesting that the present scheme is highly reliable. These energies were corrected for core−core and core−valence correlation effects using the difference between the cc-pwCVTZ/CCSD(T) all-electron energies and the cc-pVTZ/CCSD(T) valence-only energies.

Zero-point energies for methods (1) and (3) were computed using one-half the sum of the cc-pVTZ/CCSD(T) harmonic vibrational frequencies. Comparisons of the cc-pVTZ/CCSD(T) zero-point energies to experimentally-derived values for SO($X\ ^3\Sigma^-$), $H_2O(X\ ^1A_1)$, and $H_2S(X\ ^1A_1)$ suggest that no scaling of the zero-point energies is necessary for the systems studied here.[37] Individual computed harmonic vibrational frequencies for these three species differ from their experimental counterparts by at most 1%, indicating that the differences between the theoretical and experimental ZPVE's are composed solely of small anharmonic corrections.[38] Thermal corrections of enthalpies from 0 to 298.15 K were carried out using the standard ideal gas/rigid rotor/harmonic oscillator approximation.[39]

TABLE 1: Thermochemical and Spectroscopic Data (in kcal mol^{-1}) Used in the Computation of the Heat of Formation of $[2H,S,O]^+$ Isomers in This Study[a]

substance	$\Delta H_f^\circ{}_0$	$\Delta H_f^\circ{}_{298}$	IE
SO(g)	1.202 ± 0.311	1.197 ± 0.311	237.4 ± 0.1[b]
H_2S(g)	−4.2 ± 0.2	−4.9 ± 0.2	241.1 ± 0.2[c]
H_2O(g)	−57.10 ± 0.01	−57.80 ± 0.01	

[a] Enthalpies of formation are taken from the NIST-JANAF Thermochemical Tables (ref 28). [b] Reference 29. [c] Reference 30.

4. Results

4.1. Experimental Results. The $[2H,S,O]^+$ generated in reaction 3 did not react with the O_2 or with the C_2H_6 present in the flow tube ($k^{(2)} < 1 \times 10^{-13}$ cm^3 $molecule^{-1}$ s^{-1} for both reactions). However, the $C_2H_5^+$ reacted with C_2H_6, forming chiefly $C_4H_9^+$ with a bimolecular rate coefficient $k^{(2)} = 3.9 \times 10^{-11}$ cm^3 $molecule^{-1}$ s^{-1}.[10] The $C_4H_9^+$ did not react further

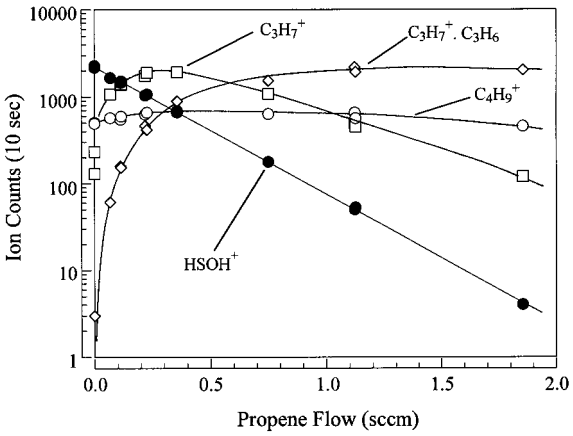

Figure 1. Variation of $HSOH^+$, $C_4H_9^+$, and ion product count rates with propene flow. The $HSOH^+$ signal decay shows excellent linearity over more than 2 orders of magnitude. The only observed primary product is $C_3H_7^+$, or protonated propene. Note the slight increase in count rate for the $C_4H_9^+$ contaminant ion at low propene flows; this effect is due to contributions from the reaction of $C_3H_7^+$ with propene. The $C_3H_7^+$ also reacts by ternary association to produce $C_3H_7^+ \cdot C_3H_6$.

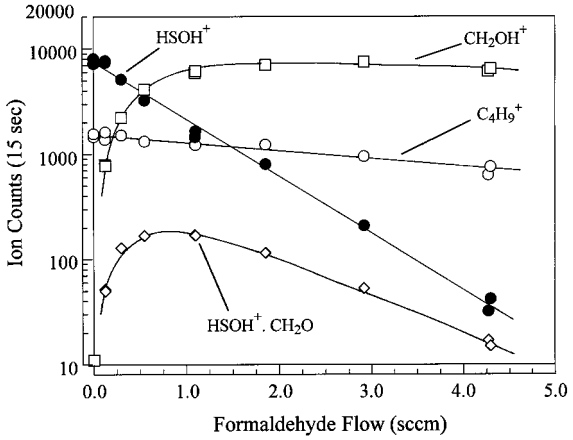

Figure 2. Variation of $HSOH^+$, $C_4H_9^+$, and ion product count rates with formaldehyde flow. Excellent linearity is observed in the $HSOH^+$ signal decay over more than 2 orders of magnitude. In this reaction, a small ternary association channel occurs in parallel with proton transfer for $HSOH^+$, with no other primary products observed. Note that the $C_4H_9^+$ is much less reactive than $HSOH^+$ with formaldehyde and does not interfere with the product determination.

appreciably, and thus enough C_2H_6 was added to establish $C_4H_9^+$ as the only other significant ion at the addition point for the reference bases. The $C_4H_9^+$ signal varied from ~9% to ~25% of the $[2H,S,O]^+$ signal during the series of experiments, as sulfurated deposits gradually accumulated in the ion source and in the SIFT. However, even at its highest contamination level the $C_4H_9^+$ never interfered critically with interpretation of the $[2H,S,O]^+$ reactivity and product formation. Other contaminant ions, largely the protonated hydrocarbons $C_nH_{2n+1}^+$ ($n = 2, 3$), were always negligible (<1%) compared to the $[2H,S,O]^+$ and the $C_4H_9^+$.

Samples of the data collected in this study are presented in Figures 1 and 2 for the reactions of $[2H,S,O]^+$ with propene and formaldehyde, respectively. The logarithmic decay of the $[2H,S,O]^+$ signal (labeled $HSOH^+$ in the figures) as a function of neutral reactant flow shows excellent linearity over more than 2 orders of magnitude in both illustrated reactions, as it does in general with the other reactant gases in this data set. This behavior implies a simple pseudo-first-order kinetic situation in which the reactivity of the entire population of $[2H,S,O]^+$ ions is well represented by a single bimolecular rate coefficient. Thus, either a single isomeric form of the $[2H,S,O]^+$ predominates or the various isomeric forms have nearly the same rate coefficients for all of their reactions with the molecules in this study (see later). It is clear from Figures 1 and 2 that the products of the $[2H,S,O]^+$ reactions are easily recognized despite the presence of $C_4H_9^+$. With propene, $[2H,S,O]^+$ reacts exclusively by proton transfer to form $C_3H_7^+$. The $C_4H_9^+$ signal actually increases at small propene flows due to the reaction of this $C_3H_7^+$ with the C_2H_6 added to the flow tube for reaction 3.[40] The $C_3H_7^+$ also reacts with propene to form a proton-bound dimer (see Figure 1). With formaldehyde, proton transfer is also a dominant reaction channel for $[2H,S,O]^+$, with a branching fraction of 0.93. A ternary association channel with a branching fraction of 0.07 at the ~0.5 Torr pressure of these experiments accounts for the remaining reaction. The $C_4H_9^+$ reaction with formaldehyde is quite slow (see Figure 2). Experimental bimolecular rate coefficients, $k_{exp}^{(2)}$, determined from data such as those illustrated in Figures 1 and 2, are presented in Table 2 for all of the reactions of $[2H,S,O]^+$ in the present study. Theoretical capture rate coefficients, $k_{TST}^{(2)}$, calculated from the variational transition state theory of Su and Chesnavich,[41] are also presented in Table 2, along with the values of the parameters (i.e., formula weight (FW), electric dipole polarizability (α), and electric dipole moment (μ)) used in these calculations.[42] Where some or all of the product is due to a termolecular process, i.e., collisional association, the $k_{exp}^{(2)}$ indicated in Table 2 represent the effective bimolecular reaction rate coefficients in ~0.5 Torr of helium. Since these associations are slow, and therefore not likely to be pressure-saturated at 0.5 Torr, the termolecular rate coefficients can be obtained simply using the expression $k_{exp}^{(3)} = k_{exp}^{(2)}/[He]$.

Overall, the reactivity of $[2H,S,O]^+$ with the reference bases is straightforward, as shown in Table 3. Three modes of reaction predominate: proton transfer (PT), charge (i.e., electron) transfer (CT), and termolecular collisional association (AS). Only in the reaction with *o*-difluorobenzene is a very small (2%) additional binary channel observed. Charge transfer effectively competes with proton transfer only in the reaction with *o*-difluorobenzene, and association is weakly competitive with proton transfer in the reactions with formaldehyde and with 1,1,1-trifluoropropanone. Binary reaction efficiency (BRE), defined as $f_b k_{exp}^{(2)}/k_{TST}^{(2)}$, where f_b is the total branching fraction of all binary channels in a reaction, decreases in a regular manner (within experimental uncertainty) with decreasing gas basicity (GB) of the reference base (see Table 3; the relative binary reaction efficiency (RBRE) is obtained by normalization of the BRE to the reaction with CH_3SH). Reaction with H_2S is by slow, hence slightly endothermic,[15] proton transfer, and no reaction is observed with c-C_6H_{12}. Below cyclohexane on the gas basicity scale, the $[2H,S,O]^+$ reacts only by slow ternary association (see Table 3).

4.2. Computational Results. Tables 4−7, respectively, summarize the high-level ab initio geometries, rotational constants, dipole moments, and harmonic vibrational frequencies for the *trans*-$HSOH^+$, *cis*-$HSOH^+$, H_2OS^+, and H_2SO^+ isomers. The variation in the bond lengths follows the expected trend as the basis set is extended and the level of electron correlation is improved, with no unusual behavior observed.[43] The ground electronic states of the vinylic isomers H_2OS^+ and H_2SO^+ are both $^2A'$, just as for the isoelectronic dihydrophosphoryl radical, H_2PO,[7] while those of the planar trans and cis isomers are $^2A''$.

Relative energies for all four $[2H,S,O]^+$ isomers are reported in Table 8 as computed using the cc-pVTZ/CCSD(T), G2, and

TABLE 2: Formula Weights (FW), Polarizabilities (α), and Electric Dipole Moments (μ) of the Indicated Reactant Reference Bases, and Calculated Collisional Rate Coefficients ($k_{TST}^{(2)}$) and Experimentally Determined Rate Coefficients ($k_{exp}^{(2)}$) for the Reactions of $HSOH^+$ with These Reference Bases at 294.5 K ± 2.5 K

reactant		FW (amu)	α^a (10^{-24} cm^3)	μ^a (D)	$10^9 k_{TST}^{(2)\,b,c}$ (cm^3 molecule^{-1} s^{-1})	$10^9 k_{exp}^{(2)\,c}$ (cm^3 molecule^{-1} s^{-1})
methanethiol	CH_3SH	48.1	5.2	1.52	1.8(7)	1.9(2)
propene	CH_2CHCH_3	42.1	6.26	0.366	1.31	1.3(2)
formic acid	HCO_2H	46.0	3.4	1.41	1.6(7)	1.5(3)
o-difluorobenzene	c-1,2-$C_6H_4F_2$	114.1	9.80	2.46	2.40	2.2(6)
1,1,1-trifluoropropanone	$CF_3C(O)CH_3$	112.1	7.8	2.90	2.6(1)	2.1(5)[d]
formaldehyde	CH_2O	30.0	2.6	2.33	2.6(5)	0.53(6)[d]
hydrogen sulfide	H_2S	34.1	3.87	0.97	1.4(8)	0.041(8)
cyclohexane	c-C_6H_{12}	84.2	10.9	0	1.37	≤0.0007
carbon disulfide	CS_2	76.1	8.8	0	1.2(6)	0.0028[d]
ethene	C_2H_4	28.1	4.25	0	1.14	0.051(0)[d]
sulfur dioxide	SO_2	64.1	4.0	1.63	1.7(6)	0.0048[d]

[a] See ref 42 for the sources of the electric dipole polarizabilities and electric dipole moments. [b] Theoretical binary reaction rate coefficients at 298 K were determined from the variational transition state theory of Su and Chesnavich (ref 41). [c] In order to avoid rounding errors, the relative binary reaction efficiencies (RBRE's) reported in Table 3 were determined using values for the theoretical and experimental binary rate coefficients to the precision indicated here, including the digits shown in parentheses, which are not significant figures of precision. [d] Effective binary rate coefficients are reported for reactions which include ternary association channels (see text).

TABLE 3: Ionization Energies (IE), Gas-Phase Basicities (GB), Proton Affinities (PA), Relative Binary Reaction Efficiencies (RBRE), Fractional Product Distributions (*f*), and Ion Products for the Reactions of $HSOH^+$ with the Indicated Reactant Reference Bases at 294.5 ± 2.5 K

reactant	IE[a] (eV)	GB[a] (kcal/mol)	PA[a] (kcal/mol)	RBRE[b]	*f*	ion product[c]
methanethiol	9.44	177.	184.8	1.00	0.98	PT
CH_3SH					0.02	CT
propene	9.73	172.7	179.6	0.98	1.00	PT
CH_2CHCH_3						
formic acid	11.33	169.8	177.3	0.89	1.00	PT
HCOOH						
o-difluorobenzene	9.29	168.1	174.8	0.92	0.49	PT
c-1,2-$C_6H_4F_2$					0.49	CT
					0.02	$C_3H_3FH^+$
1,1,1-trifluoropropanone	10.67	165.4	173.0	0.72	0.90	PT
$CF_3C(O)CH_3$					0.10	AS
formaldehyde	10.88	163.3	170.4	0.18	0.93	PT
CH_2O					0.07	AS
hydrogen sulfide	10.46	161.0	168.	0.027	1.00	PT
H_2S						
cyclohexane	9.88	159.4	164.2	≤ 0.0005	–	no reaction
c-C_6H_{12}						
carbon disulfide	10.07	157.2	163.0	zero	1.00	AS
CS_2						
ethene	10.51	155.7	162.6	zero	1.00	AS
C_2H_4						
sulfur dioxide	12.35	153.8	160.7	zero	1.00	AS
SO_2						

[a] Ionization energies (IE), gas-phase basicities (GB), and proton affinities (PA) for the reference bases are from ref 11. [b] The relative binary reaction efficiencies (RBRE) for the reactions of $HSOH^+$ with the reference bases were determined as described in the text. [c] Ion products other than the $C_3H_3FH^+$ produced in the reaction with *o*-difluorobenzene are reported by reaction type according to the following key: AS, ternary association; CT, charge transfer; PT, proton transfer.

coupled cluster CBS methods described earlier. Improvements in the level of theory serve to reduce the energy gap between the cis and trans diastereomers from ca. 3.0 kcal mol^{-1} at the cc-pVDZ/CCSD level of theory to 2.3 kcal mol^{-1} at the cc-pVTZ/CCSD(T) level. The coupled cluster CBS scheme, which is the most accurate method used here, lowers this difference to less than 2.0 kcal mol^{-1}. Of particular interest are the unexpected 3.6 kcal mol^{-1} increase (from 18.7 to 22.3 kcal mol^{-1}) and, most surprising, the 6.3 kcal mol^{-1} drop (from 36.8 to 30.5 kcal mol^{-1}) between the G2 and the coupled cluster CBS relative energies of H_2OS^+ and H_2SO^+, respectively. Several factors contribute to these differences (see Tables 6S and 7S of the Supporting Information): (1) The zero-point energy corrections for the H_2OS^+ isomer differ by a factor of almost 2 between the two methods (G2 = +0.74 kcal mol^{-1}; CBS = +1.36 kcal mol^{-1}); (2) The core-correlation correction utilized in the coupled cluster CBS scheme decreases the relative energy of the H_2SO^+ isomer by more than 2.0 kcal mol^{-1} and increases that of the H_2OS^+ isomer by nearly the same amount, indicating that core effects are substantially different between the trans isomer and the two vinylic isomers. The relative energy of the cis isomer, on the other hand, shows very little contribution from core-correlation effects; (3) improvement of the basis set from cc-pVTZ through cc-pV5Z leads to a substantial shift in the relative energies (a 2.2 kcal mol^{-1} decrease at the CCSD(T) level for H_2SO^+ and 2.4 kcal mol^{-1} at the same level for H_2OS^+) while basis-set extrapolations to infinity adjust these values by an additional kcal mol^{-1}. These data suggest that the G2 method is inadequate in this case, particularly in its corrections for basis set completeness. While it would be desirable to obtain results using even larger basis sets to refine the relative energies, it is unlikely that the CBS

TABLE 4: UHF-Based Coupled Cluster Predictions of Structural Data (Bond Lengths in Å, Angles in deg, and Rotation Constants in MHz), Dipole Moments (in D), and Harmonic Vibrational Frequencies (in cm^{-1}) for the Ground $^2A''$ State of the *trans*-HSOH Radical Cation

	cc-pVDZ		cc-pVTZ	
	CCSD	CCSD(T)	CCSD	CCSD(T)
r(H−S)	1.364	1.366	1.351	1.353
r(S−O)	1.612	1.622	1.573	1.584
r(O−H)	0.984	0.986	0.974	0.978
θ(H−S−O)	93.8	93.6	94.6	94.3
θ(S−O−H)	109.8	109.2	111.7	111.0
A_e	197885	196536	204356	202352
B_e	16700	16519	17455	17244
C_e	15400	15238	16082	15890
μ_x	−0.77	−0.71	−0.55	−0.50
μ_y	−0.46	−0.46	−0.45	−0.45
$\|\|\mu\|\|$	0.90	0.85	0.72	0.67
ω_1(a′)	3665.4	3632.5	3711.9	3665.5
ω_2(a′)	2668.3	2650.8	2638.8	2614.4
ω_3(a′)	1256.7	1248.3	1257.8	1249.6
ω_4(a′)	1006.3	994.2	1031.8	1017.8
ω_5(a′)	911.6	882.1	970.3	935.0
ω_6(a″)	626.5	630.9	610.1	612.9

TABLE 5: UHF-Based Coupled Cluster Predictions of Structural Data (Bond Lengths in Å, Angles in deg, and Rotation Constants in MHz), Dipole Moments (in D), and Harmonic Vibrational Frequencies (in cm^{-1}) for the Ground $^2A''$ State of the *cis*-HSOH Radical Cation

	cc-pVDZ		cc-pVTZ	
	CCSD	CCSD(T)	CCSD	CCSD(T)
r(H−S)	1.368	1.371	1.355	1.358
r(S−O)	1.605	1.615	1.567	1.577
r(O−H)	0.982	0.984	0.972	0.975
θ(H−S−O)	101.2	101.2	101.5	101.4
θ(S−O−H)	114.7	114.1	116.4	115.6
A_e	201021	199660	207163	205171
B_e	16665	16490	17430	17224
C_e	15389	15232	16077	15890
μ_x	−0.75	−0.70	−0.54	−0.50
μ_y	3.05	3.04	2.84	2.84
$\|\|\mu\|\|$	3.14	3.12	2.89	2.88
ω_1(a′)	3688.7	3655.9	3737.9	3692.5
ω_2(a′)	2635.2	2614.1	2610.4	2583.3
ω_3(a′)	1191.2	1181.1	1205.1	1193.9
ω_4(a′)	1003.8	987.3	1040.7	1021.4
ω_5(a′)	905.3	876.2	948.8	917.1
ω(a″)	477.3	482.9	475.6	480.7

TABLE 6: UHF-Based Coupled Cluster Predictions of Structural Data (Bond Lengths in Å, Angles in deg, and Rotation Constants in MHz), Dipole Moments (in D), and Harmonic Vibrational Frequencies (in cm^{-1}) for the Ground $^2A'$ State of the H_2OS Radical Cation

	cc-pVDZ		cc-pVTZ	
	CCSD	CCSD(T)	CCSD	CCSD(T)
r(O−S)	1.790	1.797	1.734	1.742
r(O−H)	0.981	0.983	0.971	0.974
θ(S−O−H)	117.7	117.0	119.0	118.1
θ(H−O−H)	111.9	111.6	114.4	113.9
A_e	339044	334404	352521	345713
B_e	12766	12684	13556	13455
C_e	12398	12327	13115	13030
μ_x	1.19	1.26	0.86	0.97
μ_y	3.43	3.42	3.66	3.64
$\|\|\mu\|\|$	3.63	3.65	3.76	3.76
ω_1(a′)	3640.5	3615.0	3686.4	3647.8
ω_2(a′)	1636.0	1623.3	1657.6	1637.1
ω_3(a′)	661.6	662.3	702.9	697.8
ω_4(a′)	467.6	484.4	348.2	390.8
ω_5(a″)	3751.9	3727.3	3788.6	3750.5
ω_6(a″)	917.5	913.7	930.6	924.8

TABLE 7: UHF-Based Coupled Cluster Predictions of Structural Data (Bond Lengths in Å, Angles in deg, and Rotation Constants in MHz), Dipole Moments (in D), and Harmonic Vibrational Frequencies (in cm^{-1}) for the Ground $^2A'$ State of the H_2SO Radical Cation

	cc-pVDZ		cc-pVTZ	
	CCSD	CCSD(T)	CCSD	CCSD(T)
r(S−O)	1.585	1.583	1.518	1.513
r(S−H)	1.367	1.370	1.355	1.359
θ(O−S−H)	104.4	105.0	107.0	108.1
θ(H−S−H)	99.6	99.7	101.2	101.5
A_e	148240	148498	154646	155555
B_e	17117	17129	18534	18591
C_e	16566	16560	17783	17793
μ_x	1.52	1.50	1.34	1.30
μ_y	3.49	3.50	3.52	3.57
$\|\|\mu\|\|$	3.81	3.81	3.77	3.80
ω_1(a′)	2616.7	2586.2	2574.2	2532.3
ω_2(a′)	1224.8	1215.4	1234.3	1219.3
ω_3(a′)	939.2	929.1	1018.4	1014.1
ω_4(a′)	634.8	614.1	639.0	625.0
ω_5(a″)	2650.5	2623.4	2609.6	2573.4
ω_6(a″)	908.3	895.6	937.1	918.7

data reported in Table 8 are in error by more than 1.5 kcal mol^{-1}, especially as they are relative energies.

Table 9 summarizes the computed reaction energies for both reference reactions (Schemes 1 and 2) and the associated enthalpies of formation at 0 and 298.15 K as computed for the *trans*-$HSOH^+$ isomer using the thermochemical data given in Table 1 and the energies computed as described in the Computational Methods section. Enthalpies (0 K) of formation for the other three isomers of $[2H,S,O]^+$ may be computed using the relative energies reported in Table 8. Unlike the relative energies in Table 8, basis-set effects do not appear to be as substantial for the reaction energies given in Table 9. As indicated in Tables 8S and 9S of the Supporting Information, improvement of the basis set from cc-pVTZ to cc-pV5Z at the CCSD(T) level provides an increase of less than 1.4 kcal mol^{-1} for Scheme 1 and 1.7 kcal mol^{-1} for Scheme 2. Instead, the reaction energies appear to be significantly affected by zero-point energy effects, as indicated by the more than 6.0 kcal mol^{-1} decrease in $\Delta H_{rxn,0}$ for Scheme 1 at the CCSD(T) level. The good agreement between the 0 K enthalpies of formation as computed for Schemes 1 and 2 and reported in Table 9 is encouraging, since for an exact theoretical treatment the two approaches would give identical results (to within the error bars associated with the experimental thermochemical data given in Table 1). Although a more accurate analysis of the large zero-point energy correction determined here would be desirable (using, for example, high-level coupled cluster anharmonicity calculations), it is unlikely that the exact $\Delta H_f°_0$ of the *trans*-$HSOH^+$ isomer differs by more than 1.5 kcal mol^{-1} from 190.0 kcal mol^{-1}, the average of the coupled cluster CBS results for Schemes 1 and 2.

Table 10 reports the computed proton detachment energy (PDE) of *trans*-$HSOH^+$ at various levels of theory. Of particular interest is the curious variation in the relative energies between the HSO and HOS isomers implied by the PDE values reported in the table. At the cc-pVTZ/CCSD(T) level, the two isomers are nearly degenerate, while improvement of the theoretical model to the coupled cluster CBS scheme places HSO below HOS by 7.4 kcal mol^{-1}. This result is in qualitative agreement with the findings of Xantheas and Dunning,[2f] who determined an energetic difference of 5.4 kcal mol^{-1} at the complete-basis-set CASSCF/SOCI level of theory. The ca. 2.0 kcal mol^{-1}

TABLE 8: UHF-Based Coupled Cluster, G2, and Coupled Cluster CBS Predictions of Relative Energies (in kcal mol^{-1}) for Selected Structural Isomers of the [2H,S,O]$^+$ Radical, Zero-Point-Corrected Values for the Coupled Cluster Methods (in Parentheses)

		cc-pVDZ		cc-pVTZ			coupled
isomer	state	CCSD	CCSD(T)	CCSD	CCSD(T)	G2	cluster CBS
t-HSOH$^+$	^{2}A″	0.0 (0.0)	0.0 (0.0)	0.0 (0.0)	0.0 (0.0)	0.0	0.0
c-HSOH$^+$	^{2}A″	3.2 (2.9)	3.3 (2.9)	2.5 (2.2)	2.6 (2.3)	2.1	1.9
H_2OS^+	^{2}A′	10.2 (11.5)	12.8 (14.0)	14.6 (15.9)	16.1 (17.5)	18.7	22.3
H_2SO^+	^{2}A′	37.9 (36.2)	38.5 (36.8)	36.8 (35.1)	37.3 (35.6)	36.8	30.5

TABLE 9: Enthalpies of Reaction for Schemes 1 and 2 and the Associated Enthalpies of Formation (in kcal mol^{-1}) of the *trans*-HSOH Radical Cation As Computed Using cc-pVTZ/CCSD(T), G2, and Coupled Cluster CBS Approaches Described in the Text

t-HSOH$^+$(g) → H_2(g) + SO$^+$(g)	$\Delta H_{rxn,0}$	$\Delta H_{rxn,298}$	$\Delta H_f°_0$	$\Delta H_f°_{298}$
cc-pVTZ/CCSD(T)	49.0	50.6	189.6	188.0
G2	47.8	49.4	190.8	189.2
coupled cluster CBS	48.3	49.9	190.3	188.7
2*t*-HSOH$^+$(g) → H_2S^+ + H_2O(g) + SO$^+$(g)	$\Delta H_{rxn,0}$	$\Delta H_{rxn,298}$	$\Delta H_f°_0$	$\Delta H_f°_{298}$
cc-pVTZ/CCSD(T)	37.6	39.4	190.4	188.8
G2	36.2	37.9	191.1	189.6
coupled cluster CBS	39.0	40.8	189.7	188.1

TABLE 10: Proton-Detachment Enthalpies (in kcal mol^{-1}) Leading to HSO and HOS of *trans*-HSOH$^+$ As Computed Using the cc-pVTZ/CCSD(T), G2, and Coupled Cluster CBS Methods Described in the Text

	t-HSOH$^+$ → HSO + H$^+$		*t*-HSOH$^+$ → HOS + H$^+$	
	$\Delta H_{rxn,0}$	$\Delta H_{rxn,298}$	$\Delta H_{rxn,0}$	$\Delta H_{rxn,298}$
cc-pVTZ/CCSD(T)	176.2	176.0	176.2	176.1
G2	170.0	169.9	174.0	173.8
coupled cluster CBS	168.1	167.9	175.5	175.4

TABLE 11: Energy (in kcal mol^{-1}) of HOS Relative to HSO as a Function of Basis Set, Level of Correlation, and Other Corrections[a]

	UHF	CCSD	CCSD(T)
cc-pVDZ	−8.40	−7.49	−6.96
cc-pVTZ	−4.11	−2.75	−2.26
cc-pVQZ	−2.78	−0.75	−0.17
cc-PV5Z	−1.75	0.74	1.41
∞	−0.74	1.97	2.67
+core[b]		4.73	5.57
+ZPVE[c]		6.59	7.43
+298 K[d]		6.60	7.44

[a] See the discussions in the text for an explanation of the basis-set extrapolations used to obtain the infinite basis-set results. [b] Plus core-correlation corrections. [c] Plus zero-point energy corrections. [d] Plus thermal corrections.

difference between the SOCI and the coupled cluster CBS relative energies is most likely due to the inclusion of core-correlation effects in the CBS approach used here; as indicated in Table 11, core effects contribute more than 2.5 kcal mol^{-1} to the final relative energy. Of concern, however, is the significant difference (0.7 kcal mol^{-1}) in core-correlation effects between the cc-pwCVTZ and cc-pCVTZ basis sets. For other species examined in this work, the largest such difference is 0.4 kcal mol^{-1}, with most species exhibiting only a 0.03 kcal mol^{-1} difference. The larger difference for the HSO/HOS relative energies suggests that more caution is required to accurately account for core-correlation effects in these species. Hence, the PDE's given in Table 10 must be considered somewhat less reliable (perhaps by 1.5 kcal mol^{-1}) than the relative energies and enthalpies of formation given in Tables 8 and 11, respectively. Zero-point vibrational energy corrections, which are nearly identical to those used in the Xantheas and Dunning study,[2f] account for slightly less than 2.0 kcal mol^{-1} of the final PDE's, as indicated in Table 11. We therefore expect the proton detachment energies given in Table 10 to be accurate to within 3.0 kcal mol^{-1}.

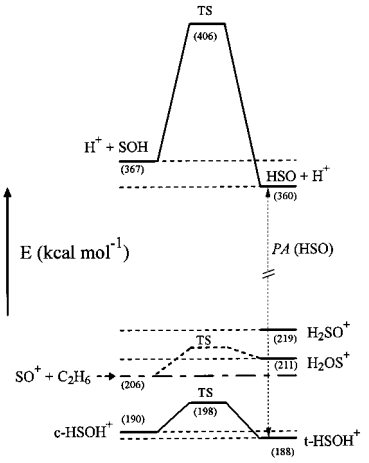

Figure 3. Energy diagram for the various [2H,S,O]$^+$ isomers and their products of proton detachment. Numbers in parentheses indicate estimated energies, to the nearest kcal mol^{-1}, of the isomers and transition states (TS) relative to the elemental standard states at 298 K. Data for the energy of ground-state HSO and the HSO ↔ HOS isomerization barrier are taken from ref 2f; data for the [2H,S,O]$^+$ isomers and the HSO/HOS energy separation are from the coupled cluster CBS calculations of the present work. Other thermochemical data used to construct the figure are taken from ref 11. Indicated in the figure is the reaction enthalpy, relative to elemental standard states at 298 K, available to form [2H,S,O]$^+$ in reaction 3 (see text). The energy barrier for reaction 3 was not calculated, but is indicated by the TS drawn with a dotted line. Also indicated is the "true" proton affinity (PA) of HSO, which corresponds to the energy of proton detachment from *trans*-HSOH$^+$, the lowest-energy [2H,S,O]$^+$ isomer.

5. Discussion

5.1. Isomeric Forms of [2H,S,O]$^+$. The reactivity demonstrated by the [2H,S,O]$^+$ ions generated from reaction 3, combined with the coupled cluster ab initio results, and energetic and mechanistic information based on reactions 2 and 3, provides compelling evidence that these ions are entirely of the H−S−O−H connectivity. The available enthalpy (calculated from the values of $\Delta H_f°_{298}$ for the reactants and products[11]) to create the [2H,S,O]$^+$ in reaction 3 is ∼206 kcal mol^{-1}. The estimated $\Delta H_f°_{298}$ of the sulfoxide isomer, H_2SO^+, however, is 218.9 ± 2.1 kcal mol^{-1},[44] and thus the formation of H_2SO^+ by reaction 3 is energetically forbidden by at least 10.8 kcal mol^{-1} (see Figure 3).[45] Moreover, any available excess energy, either from residual excitation in the SO$^+$(X $^2\Pi_r$) or from the high-energy tail of the Maxwell−Boltzmann energy distribution for the He carrier gas at ∼294.5 K, is insufficient to drive the formation of H_2SO^+. Note, too, that reaction 3 is rapid, with a rate coefficient slightly above the theoretical value of 1.1 ×

SCHEME 3

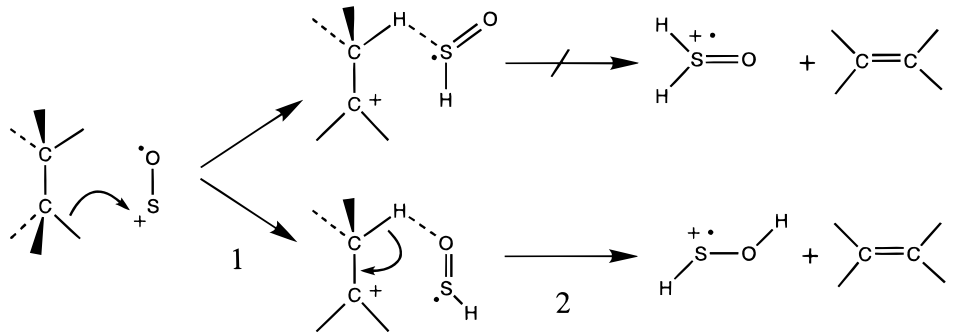

10^{-9} cm^3 molecule^{-1} s^{-1},[4a] and thus is not subject to energetic constraints. Therefore, we can confidently rule out the formation of H_2SO^+ in this reaction.

Formation of the ylide isomer, with $\Delta H_f°_{298}(H_2OS^+) = 210.8 \pm 2.1$ kcal mol^{-1},[44] is endothermic by at least 2.7 kcal mol^{-1}. Therefore, although the energetics implies that H_2OS^+ is not formed in reaction 3, the argument is weaker than with H_2SO^+, and we consider additional evidence for this conclusion. For example, a charge (electron) transfer channel occurs in the reactions of the [2H,S,O]$^+$ ions with methanethiol (IE = 9.44 eV) and with *o*-difluorobenzene (IE = 9.29 eV), and is a major product channel in the latter case (see Table 3). The computed recombination energies (RE's) of the H_2OS^+ and *trans*-HSOH$^+$ isomers are 8.6 ± 0.1 and 9.5 ± 0.1 eV, respectively, at the G2 level of theory.[46] Thus, electron transfer to H_2OS^+ is substantially endothermic with methanethiol and *o*-difluorobenzene, and cannot occur unless driven by isomerization to the H−S−O−H connectivity during the interaction. Such a process would require an intimate encounter rather than a long-range electron jump and would be unlikely to compete effectively with the mechanistically simpler proton transfer.

Conversely, the computed recombination energies of the HSOH$^+$ diastereomers are consistent with the observed charge-transfer behavior. Note that the [2H,S,O]$^+$ ions are unreactive with cyclohexane (IE < 9.9 eV[11]). Assuming that reaction actually does occur, entirely by endothermic charge transfer with an efficiency of $\epsilon = 5 \times 10^{-4}$ (see Table 3), the Boltzmann expression $\epsilon = \exp(-E_a/k_BT)$ implies a lower-limit charge-transfer endothermicity of $E_a = 0.2$ eV at the experimental temperature. Thus, the RE of the experimentally-observed [2H,S,O]$^+$ ions is <9.7 eV. The substantial charge-transfer channel in the rapid reaction with o-difluorobenzene (IE = 9.29 eV[11]) places the lower limit of this RE at 9.3 eV. Noting the observed small charge-transfer channel with methanethiol (IE = 9.44 eV), we infer a range of 9.5 ± 0.2 eV for the RE of the [2H,S,O]$^+$ ions generated in reaction 3. This range is clearly most consistent with the HSOH$^+$ diastereomers[46] (see above).

It might be argued that, since only 49% of the product with *o*-difluorobenzene is due to charge transfer, as much as 51% of the total product could arise from reactions involving H_2OS^+. However, this is unlikely, since the large difference in enthalpy of formation between H_2OS^+ and the two HOSH$^+$ isomers reflects the larger proton affinity (i.e., by >20 kcal mol^{-1}) of HOS at the sulfur atom versus the oxygen atom (see Figure 3). Substantial populations of both H_2OS^+ and the HOSH$^+$ diastereomers would therefore lead to bimodal decays of the [2H,S,O]$^+$ ions for reference bases with proton affinities higher than the proton detachment energy of H_2OS^+, but lower than those of the HOSH$^+$ isomers. The fact that the logarithmic decays of the [2H,S,O]$^+$ ions are quite linear for the slow reactions in the present data set therefore suggests that the HSOH$^+$ isomers, which are expected to react similarly, are the only isomeric forms of [2H,S,O]$^+$ formed in reaction 3.

Further evidence for the nonformation of H_2OS^+ is obtained from the probable two-step mechanism of reaction 3[4a] (see Scheme 3). At the cc-pVTZ/CCSD(T) level of theory, $SO^+(X\ ^2\Pi_r)$ has a Mulliken charge of 0.693 on the S atom and 0.307 on the O atom. Thus, the ion−induced dipole interaction which forms the reactive complex is stronger with the sulfur terminus than with the oxygen terminus of $SO^+(X\ ^2\Pi_r)$. Inductive C−H bond cleavage should then preferentially be initiated by the sulfur terminus and thereby form HSO rather than HOS. If such is the case, then the second step of Scheme 3, which involves an intramolecular proton transfer, necessarily has to generate one or both of the HSOH$^+$ diastereomers, since formation of H_2SO^+ is quite endothermic (see above). Even if HOS were formed in the first step, the activation barrier for protonation at the oxygen atom is likely to be high enough to impede this process, since formation of H_2OS^+ is slightly endothermic for reaction 3 (see above and Figure 3). The fact that reaction 3 proceeds at the collisional rate, with [2H,S,O]$^+$ representing 80% of the ion product, implies that such a barrier has little or no influence. Furthermore, the proton affinity of HOS at the oxygen atom is several kcal mol^{-1} lower than that of the C_2H_4 leaving partner (PA[14] = 163 kcal mol^{-1}),[47] making the intramolecular proton transfer to form H_2OS^+ unlikely.

Altogether, the evidence presented above indicates beyond a reasonable doubt that only the two HSOH$^+$ diastereomers are generated in reaction 3. Whether the cis or the trans diastereomer or a mixture of the two predominates could not be determined conclusively in this study (however, see below). At the coupled cluster CBS level of theory, the cis isomer lies some 1.9 kcal mol^{-1} above the trans isomer (see Table 8). Low levels (i.e., cc-pVDZ/CCSD(T)) of theory predict a cis−trans isomerization barrier of 8.1 kcal mol^{-1} measured from the cis side. The enthalpy of reaction 3 is sufficient to drive the cis ↔ trans interconversion if more than half of that energy is accessible to the isomerization process (see Figure 3). Therefore, regardless of which diastereomer is preferentially formed initially, the reaction enthalpy is sufficient to scramble this information prior to the removal of internal energy from the HSOH$^+$ by collisions with the He carrier gas, which occurs on a ~200 ns time scale under our experimental conditions. After removal of internal excitation by the He, the computed cis ↔ trans isomerization barrier effectively prevents further interconversion at the experimental temperature of 294.5 ± 2.5 K.

5.2. Gas Basicity and Proton Affinity of HSO. A proton can be removed from either the oxygen or the sulfur atom of HSOH$^+$, forming HSO or HOS, respectively. For a given diastereomer of HSOH$^+$, deprotonation at the oxygen atom is more exothermic than sulfur deprotonation by $\Delta H_f°_{298}(HSO) - \Delta H_f°_{298}(SOH) = 7.4$ kcal mol^{-1} (see Figure 3). Unless steric

or other exceptional constraints are in effect, proton transfer generally proceeds rapidly when it is exothermic by more than a few kcal mol^{-1}.[15,48] When S-deprotonation to form HOS is slightly endothermic, and hence inefficient, O-deprotonation to form HSO is still appreciably exothermic and proceeds rapidly. Only as O-deprotonation approaches thermoneutrality does the overall reaction become inefficient. Therefore, the thermokinetic bracketing method employed here measures the gas-phase basicity of HSO, i.e., the thioperoxy radical, rather than that of HOS.

Bouchoux et al. have developed a simple model to describe the correlation between $k_{exp}^{(2)}$ and the standard free energy, $\Delta G°$, for proton-transfer reactions at low pressure ($\leq 3 \times 10^{-4}$ Torr).[15] The kinetic and reactive processes considered in this model are

$$[XH]^+ + B \underset{k_{-1}}{\overset{k_{TST}}{\rightleftharpoons}} [XHB]^{+}* \xrightarrow{k_1} X + [BH]^+ \qquad (6)$$

where X represents the protonated radical (HSO in the present case) and B represents the reference base. Reactions with prominent binary channels other than proton transfer (e.g., the 49% charge-transfer channel with *o*-difluorobenzene; see Table 3) are not considered and therefore cannot be interpreted using the Bouchoux model. Ternary association channels, which represent collisional stabilization of the activated $[XHB]^{+}*$ complex by a third body, also are not considered by the low-pressure Bouchoux model.[15] At our experimental pressure of ~0.5 Torr, however, association frequently is observed, notably in parallel with proton transfer when the reference base has a gas-phase basicity comparable to that of the species under investigation. Such behavior is observed with $HSOH^+$ in the present study (see Table 3) and with $HSSH^+$ in our previous study.[16] The observed associated product arises from ion complexes for which unimolecular dissociation, governed by the rate coefficients k_1 and k_{-1} in eq 6, is inefficient relative to stabilization by collisions with the He carrier gas under our experimental conditions (see above). However, Bouchoux et al. assume that the $[XHB]^{+}*$ complex is highly reactive (i.e., either k_1 or k_{-1} in eq 6, or both, are of the same order as k_{TST}) in order to derive a simple expression for the reaction efficiency.[15] Association channels represent the population of $[XHB]^{+}*$ that is not highly reactive, and these should therefore be excluded from the thermokinetic analysis. Thus, we employ the relative binary reaction efficiencies (RBRE's) as described above, omitting contributions to the reactivity from ternary association.[49]

A plot of RBRE versus −GB(B), where the GB(B) are the gas-phase basicities of the reference bases taken from the most recent NIST compilation (see Table 3),[14] is presented in Figure 4 for the reactions of $HSOH^+$ and those of $HSSH^+$ for comparison. Two modifications to the thermokinetic plot from our previous study[16] have been made for the reactions of $HSSH^+$: first, a data point has been added for the reaction with 1,1,1-trifluoropropanone (GB = 165.4 kcal mol^{-1}), which proceeds entirely by association and therefore has a RBRE of zero; second, the data point for the reaction with *trans*-2-butene (GB = 171.6 kcal mol^{-1}) has been omitted because its anomalously large rate coefficient implies that the reaction proceeds not by simple proton transfer forming *sec*-$C_4H_9^+$, but rather is driven by isomerization to form *tert*-$C_4H_9^+$.[50,51] The three-parameter fits to the thermokinetic data shown in Figure 4 are from the relationship between reaction efficiency and GB(B) derived by Bouchoux et al.:[15]

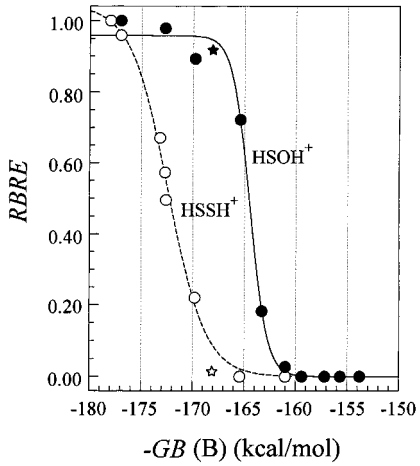

Figure 4. Plots of the relative binary reaction efficiencies (RBRE, defined in the text) as a function of negative gas-phase basicities (−GB) of the corresponding reference bases for the proton-transfer reactions of $HSSH^+$ in ref 16 and $HSOH^+$ in the present work. The fits to the thermokinetic data are from the model of Bouchoux et al. (ref 15). The plot for the $HSSH^+$ data is revised from that presented in ref 16 (see text). Stars indicate data for which an appreciable (>2%) binary channel *other* than proton transfer occurs; these data are not included in the fit, as discussed in the text.

$$\mathrm{RBRE} = \frac{1}{1 + e^{(\Delta G^0 + \Delta G_a{}^0)/R_g T}} = \frac{a}{1 + e^{[b(-\mathrm{GB(B)}+c)]}} \qquad (7)$$

In eq 7, R_g is the gas constant and $\Delta G_a°$ is interpreted by Bouchoux et al. as an "intrinsic barrier" which is probably small and nearly constant for proton-transfer reactions.[15] The desired gas-phase basicity, GB(X) (X = HSO, HS_2), is obtained from the fit as GB(X) = $c - 1/b$. The fits to the data for $HSOH^+$ and $HSSH^+$ yield gas-phase basicities of 163.6 ± 2.2 and 170.6 ± 2.2 kcal mol^{-1} for HSO and HS_2, respectively;[52] this revised value for GB(HS_2,298 K) from the improved data fit is 0.8 kcal mol^{-1} higher than our previous determination.[16]

When a species upon protonation can form two or more stable isomers with different enthalpies of formation, each isomer corresponds to a different GB and PA for the species. For example, protonation of CO can occur at the carbon or the oxygen atom, with very different values of GB and PA at these two sites.[14] The situation is more complex for HSO, which has four stable protonated forms (i.e., H_2SO^+, H_2OS^+, *cis*-$HSOH^+$, and *trans*-$HSOH^+$). The values of GB and PA which are generally of principal interest are those corresponding to the lowest-energy protonated isomer, i.e., *trans*-$HSOH^+$ in the present case (see Figure 3). However, as discussed above, both diastereomers of $HSOH^+$ may be formed in reaction 3, and their proportions in the flow tube are unknown. Unlike the case with H_2OS^+ discussed above, the computed energy difference of 1.9 kcal mol^{-1} between the two $HSOH^+$ diastereomers (see Table 8) is too small for sensitive discrimination between these isomers based on the observed reactivity. If we simply assume that the $HSOH^+$ formed consists entirely of the trans diastereomer, the value for GB(HSO,298 K) obtained from the fit to eq 7 is then equal to the "true" gas basicity of HSO, i.e., the value corresponding to the most thermodynamically stable protonated isomer. Such an assumption places additional uncertainty corresponding to the energy separation between the cis and trans diastereomers on the upper-limit uncertainty of the reported value. Thus, in order to account for the possibility that the reacting $HSOH^+$ consists entirely of the cis isomer, contrary to our assumption, we report a value of 163.6 (+4.6, −2.2) kcal mol^{-1} for GB(HSO,298 K).[53]

The proton affinity of HSO is obtained from the corresponding gas-phase basicity by adding the entropic contribution due to the removal of a proton from $HSOH^+$:

$$PA(HSO,T) = GB(HSO,T) + T[S°(H^+,T) + S°(HSO,T) - S°(HSOH^+,T)] \quad (8)$$

The protonation entropy is defined by the last two terms of eq 8, viz., $\Delta S_p(HSO,T) = S°(HSOH^+,T) - S°(HSO,T)$.[14] When, as in the present case, the van't Hoff method cannot be used to measure the entropy change experimentally, one must resort to an estimate or a calculation. A commonly-used simplification[14] is to assume that the change in rotational symmetry number accounts for most of the protonation entropy, which is thus expressed as

$$\Delta S_p(HSO) \approx R_g \ln[\sigma(HSO)/\sigma(HSOH^+)] = R_g \ln(1/1) = 0 \quad (9)$$

Within this approximation, PA(HSO,298 K) = 171.4 (+4.7, −2.4) kcal mol^{-1}, where $S°(H^+,298\ K)$ is calculated from the Sackur−Tetrode equation.[38] Using the same approximation for HS_2, with $\sigma(HS_2) = 1$ and $\sigma(HSSH^+) = 2$, we obtain a value for PA(HS_2,298 K) of 178.8 ± 2.4 kcal mol^{-1} from the revised value of GB(HS_2,298 K) presented above. From this value for PA(HS_2,298 K) and the known values of $\Delta H_f°_{298}(H^+)$[11] and $\Delta H_f°_{298}$(*trans*-HS_2H^+),[54] $\Delta H_f°_{298}(HS_2)$ is determined to be 25.8 ± 2.5 kcal mol^{-1}, 0.8 kcal mol^{-1} higher than reported in our previous study.[16] We have assumed here that the $HSSH^+$ generated in that study was entirely of the trans diastereomer, because formation of the cis diastereomer in the reaction of S_2^+ with C_2H_6 is endothermic by ∼1.6 kcal mol^{-1} and probably proceeds through an activation barrier (see section 5.1).

Using the rotation constant and harmonic vibrational frequencies that we have determined for HSO (see Supporting Information) and the two $HSOH^+$ diastereomers (see Tables 4 and 5) at the cc-pVTZ/CCSD(T) level of theory, we can calculate ΔS_p(HSO) directly from the full classical partition function.[38,55] The corrections to eq 9 from this calculation are small but nontrivial: for protonation of HSO to *trans*-$HSOH^+$ at 298 K, $T\Delta S_p$ = 0.4 kcal mol^{-1}; for protonation to *cis*-$HSOH^+$ at 298 K, $T\Delta S_p$ = 0.5 kcal mol^{-1}.[56] Therefore, assuming as before that the $HSOH^+$ generated is entirely of the trans variety, our best value for PA(HSO,298 K) is 171.0 (+4.6, −2.4) kcal mol^{-1}. Our best value for PA(HS_2,298 K) is 178.8 ± 2.4 kcal mol^{-1} as above, although a calculation of $\Delta S_p(HS_2)$ using the full partition function is likely to adjust this value very slightly downward, analogous to the situation for HSO.

If it could be known with absolute certainty that reaction 3 produced the *trans*-$HSOH^+$ diastereomer exclusively, we could report that PA(HSO,298 K) = 171.0 ± 2.4 kcal mol^{-1}, with a symmetric uncertainty interval as we have done with PA(HS_2,298 K). Then from the energy-balanced equation

$$\Delta H_f°_{298}(HSOH^+) = \Delta H_f°_{298}(H^+) + \Delta H_f°_{298}(HSO) - PA(HSO,298\ K) \quad (10)$$

using our value for PA(HSO,298 K) along with $\Delta H_f°_{298}(H^+)$ = 365.7 kcal mol^{-1} (with negligible uncertainty)[11] and $\Delta H_f°_{298}$(HSO) = −6.1 ± 1.3 kcal mol^{-1},[2f] we would obtain a value for $\Delta H_f°_{298}(HSOH^+)$ = 188.6 ± 2.7 kcal mol^{-1}, in superb agreement with the value of 188.4 ± 1.5 kcal mol^{-1} obtained for *trans*-$HSOH^+$ from the average of our two coupled cluster CBS determinations (see Table 9). This implies that the *trans*-$HSOH^+$ diastereomer is the dominant, if not the only, isomer present in the bracketing reactions. However, the energy separation of 1.9 kcal mol^{-1} between the cis and trans isomers is smaller than the uncertainties involved in this calculation, and we therefore cannot make this conclusion with absolute confidence.

6. Summary and Conclusions

Ions with the empirical formula $[2H,S,O]^+$ were generated by the reaction of $SO^+(X\ ^2\Pi_r)$ with C_2H_6 under thermal conditions in a SIFT. These ions were reacted with a series of reference bases in order to measure their free energy of proton detachment by the thermokinetic bracketing method of Bouchoux et al.[15] A parallel ab initio study of the thermodynamically stable $[2H,S,O]^+$ and the [2H,S,O] isomers, as well as the related neutral radicals HSO and HOS, was conducted at various levels of theory, including coupled cluster and Gaussian-2 methodologies, in order to determine the enthalpies of formation and other thermochemical properties of the cation species. These data suggest that the cis and/or trans diastereomer of $HSOH^+$ is the only isomer of $[2H,S,O]^+$ produced in the experiment. In agreement with previous theoretical analyses,[2f] accurate prediction of the relative energies of neutral HSO and HOS is found to require high levels of theory, with careful consideration of core-correlation, basis-set, and zero-point effects.

The thermokinetic bracketing analysis, interpreted in light of the ab initio results, yields a gas-phase basicity of GB(HSO,298 K) = 163.6 (+4.6, −2.2) kcal mol^{-1} for protonation of HSO to the *trans*-$HSOH^+$ isomer, where the asymmetric uncertainty interval reflects the possibility that the $HSOH^+$ generated in the experiment is entirely of the cis form, which lies only 1.9 kcal mol^{-1} above the trans form according to our coupled cluster CBS computations. Using rotational constants and harmonic vibrational frequencies generated in our ab initio study, the entropic contribution to the gas-phase basicity of HSO was calculated, yielding a proton affinity of PA(HSO,298 K) = 171.0 (+4.6, −2.4) kcal mol^{-1}. Assuming that we know, a priori, that only *trans*-$HSOH^+$ is present for reaction with the reference bases, we can write PA(HSO,298 K) as 171.0 ± 2.4 kcal mol^{-1}, from which we deduce a value for $\Delta H_f°_{298}$(*trans*-$HSOH^+$) of 188.6 ± 2.7 kcal mol^{-1}, in excellent agreement with the predicted value of 188.4 ± 1.5 kcal mol^{-1} at our highest level of ab initio theory. We therefore suggest that the experiment measures the "true" proton affinity of HSO, i.e., protonation to form *trans*-$HSOH^+$, the lowest-energy isomer in the $[2H,S,O]^+$ family.

Finally, revised values of GB(HS_2,298 K) = 170.6 ± 2.2 kcal mol^{-1}, PA(HS_2,298 K) = 178.8 ± 2.4 kcal mol^{-1}, and $\Delta H_f°_{298}(HS_2)$ = 25.8 ± 2.5 kcal mol^{-1} were determined from a reanalysis of our previous thermokinetic bracketing study of the proton-transfer reactions of $HSSH^+$.[16]

Acknowledgment. N.G.A. gratefully acknowledges the National Science Foundation, Division of Astronomical Sciences, under grant AST-9415485. Contributions by T.D.C. and H.F.S. were supported by the National Science Foundation, Division of Chemistry, under grant CHE-9815397. We thank Roger Grev (Kentucky), Wesley D. Allen (Georgia), Atilla Császár (Budapest), and David Feller (Pacific Northwest National Laboratories) for helpful discussions and for their recommendations regarding reference Schemes 1 and 2 for the heat of formation computations. We are also very grateful to Kirk Peterson and Thom Dunning (Pacific Northwest National Laboratories) for providing the cc-pCVDZ, cc-pwCVDZ, cc-

pCVTZ, and cc-pwCVTZ basis sets for sulfur and the cc-pwCVDZ and cc-pwCVTZ basis sets for oxygen prior to publication.

Supporting Information Available: Tables of complete theoretical geometries, dipole moments, and harmonic vibrational frequencies for the neutral [2H,S,O] and [H,S,O] species. Tables of the energies of H_2OS^+ and H_2SO^+ relative to *trans*-$HSOH^+$ and reaction energies for Schemes (1) and (2) and *trans*-$HSOH^+$ as a function of basis set, level of correlation, and other corrections. This material is available free of charge via the Internet at http://pubs.acs.org.

References and Notes

(1) (a) Balucani, N.; Casavecchia, P.; Stranges, D.; Volpi, G. G. *Chem. Phys. Lett.* **1993**, *211*, 469. (b) O'Hair, R. A. J.; DePuy, C. H.; Bierbaum, V. M. *J. Phys. Chem.* **1993**, *97*, 7955. (c) Davidson, F. E.; Clemo, A. R.; Duncan, G. L.; Browett, R. J.; Hobson, J. H.; Grice, R. *Mol. Phys.* **1982**, *46*, 33. (d) Slagle, I. R.; Baiocchi, F.; Gutman, D. *J. Phys. Chem.* **1978**, *82*, 1333. (e) Schurath, U.; Weber, M.; Becker, K. H. *J. Chem. Phys.* **1977**, *67*, 110. (f) Cheng, B.-M.; Chew, E. P.; Hung, W.-C.; Eberhard, J.; Lee, Y.-P. *J. Synchrotron Radiat.* **1998**, *5*, 1041. (g) Quandt, R. W.; Wang, X.; Tsukiyama, K.; Bersohn, R. *Chem. Phys. Lett.* **1997**, *276*, 122. (h) Cheng, B.-M.; Eberhard, J.; Chen, W.-C.; Yu, C.-h. *J. Chem. Phys.* **1997**, *106*, 9727. (i) Yasunori, Y.; Kasai, T.; Ohoyama, H.; Kuwata, K. *Can. J. Chem.* **1995**, *73*, 204. (j) Iraqi, M.; Goldberg, N.; Schwarz, H. *J. Phys. Chem.* **1994**, *98*, 2015. (k) Ravichandran, K.; Williams, R.; Fletcher, T. R. *Chem. Phys. Lett.* **1994**, *217*, 375. (l) Lee, Y.-Y.; Lee, Y.-P.; Wang, N. S. *J. Chem. Phys.* **1994**, *100*, 387. (m) Hung, W.-C.; Lee, Y.-P. *J. Chin. Chem. Soc.* **1993**, *40*, 407. (n) Wang, N. S.; Howard, C. J. *J. Phys. Chem.* **1990**, *94*, 8787. (o) Lovejoy, E. R.; Wang, N. S.; Howard, C. J. *J. Phys. Chem.* **1987**, *91*, 5749. (p) Kendall, D. J. W.; O'Brien, J. J. A.; Sloan, J. J.; Macdonald, R. G. *Chem. Phys. Lett.* **1984**, *110*, 183. (q) Satoh, M.; Ohashi, N.; Matsuoka, S. *Bull. Chem. Soc. Jpn.* **1983**, *56*, 2545. (r) Sears, T. J.; McKellar, A. R. W. *Mol. Phys.* **1983**, *49*, 25. (s) Kawasaki, M.; Kasatani, K.; Tanahashi, S.; Sato, H. *J. Chem. Phys.* **1983**, *78*, 7146. (t) Webster, C. R.; Brucat, P. J.; Zare, R. N. *J. Mol. Spectrosc.* **1982**, *92*, 184. (u) Endo, Y.; Saito, S.; Hirota, E. *J. Chem. Phys.* **1981**, *75*, 4379. (v) Ohashi, N.; Kakimoto, M.; Saito, S.; Hirota, E. *J. Mol. Spectrosc.* **1980**, *84*, 204. (w) Kakimoto, M.; Saito, S.; Hirota, E. *J. Mol. Spectrosc.* **1980**, *80*, 334. (x) Kawasaki, M.; Kasatani, K.; Sato, H. *Chem. Phys. Lett.* **1980**, *75*, 128.

(2) (a) Goumri, A.; Laakso, D.; Rocha, J.-D. R.; Smith, C. E.; Marshall, P. *J. Chem. Phys.* **1995**, *102*, 161. (b) Wilson, C.; Hirst, D. M. *J. Chem. Soc., Faraday Trans.* **1994**, *90*, 3051. (c) Esseffar, M.; Mó, O.; Yáñez, M. *J. Chem. Phys.* **1994**, *101*, 2175. (d) Espinosa-Garcia, J.; Corchado, J. C. *Chem. Phys. Lett.* **1994**, *218*, 128. (e) Morris, V. R.; Jackson, W. M. *Chem. Phys. Lett.* **1994**, *223*, 445. (f) Xantheas, S. S.; Dunning, T. H., Jr. *J. Phys. Chem.* **1993**, *97*, 6616. (g) Xantheas, S. S.; Dunning, T. H., Jr. *J. Phys. Chem.* **1993**, *97*, 18. (h) Plummer, P. M. *J. Chem. Phys.* **1990**, *92*, 6627. (i) Luke, B. T.; McLean, A. D. *J. Phys. Chem.* **1985**, *89*, 4592. (j) Buenker, R. J.; Bruna, P. J.; Peyerimhoff, S. D. *Isr. J. Chem.* **1980**, *19*, 309. (k) Hinchliffe, A. *J. Mol. Struct.* **1980**, *66*, 235. (l) Sannigrahi, A. B. *J. Mol. Struct.* **1978**, *44*, 223. (m) White, J. N.; Gardiner, W. C., Jr. *Chem. Phys. Lett.* **1978**, *58*, 470. (n) Benson, S. W. *Chem. Rev.* **1978**, *78*, 23. (o) Sannigrahi, A. B.; Peyerimhoff, S. D.; Buenker, R. J. *Chem. Phys.* **1977**, *20*, 381.

(3) Tyndall, G. S.; Ravishankara, A. R. *Int. J. Chem. Kinet.* **1991**, *23*, 483−527.

(4) (a) Decker, B. K.; Adams, N. G.; Babcock, L. M. *Int. J. Mass Spectrom.* **2000**, *195/196*, 185−201. (b) Decker, B. K.; Babcock, L. M.; Adams, N. G. *J. Phys. Chem. A* **2000**, *104*, 801−810. (c) Adams, N. G.; Williams, T. L.; Babcock, L. M.; Decker, B. K. *Recent Res. Devel. Phys. Chem.* **1999**, *3*, 191.

(5) Turner, B. E. *Astrophys. J.* **1994**, *430*, 727−742.

(6) (a) Cárdenas-Jirón, G. I.; Toro-Labbé, A. *J. Mol. Struct.* **1997**, *390*, 79. (b) Goumri, A.; Rocha, J.-D. R.; Laakso, D.; Smith, C. E.; Marshall, P. *J. Chem. Phys.* **1994**, *101*, 9405. (c) Wolfe, S.; Schlegel, H. B. *Gazz. Chim. Ital.* **1990**, *120*, 285. (d) Solà, M.; Gonzalez, C.; Tonachini, G.; Schlegel, H. B. *Theor. Chim. Acta* **1990**, *77*, 281. (e) Wallmeier, H.; Kutzelnigg, W. *J. Am. Chem. Soc.* **1979**, *101*, 2084. (f) Lee, T. J.; Handy, N. C.; Rice, J. E.; Scheiner, A. C.; Schaefer, H. F. *J. Chem. Phys.* **1986**, *85*, 3930. (g) Magnusson, E. *Aust. J. Chem.* **1986**, *39*, 735. (h) Magnusson, E. *Tetrahedron* **1985**, *41*, 2939. (i) Magnusson, E. *J. Comput. Chem.* **1984**, *5*, 612.

(7) Wesolowski, S. S.; Johnson, E. M.; Leininger, M. L.; Crawford, T. D.; Schaefer, H. F. *J. Chem. Phys.* **1998**, *109*, 2694.

(8) Smardzewski, R. R.; Lin, M. C. *J. Chem. Phys.* **1977**, *66*, 3197.

(9) Iraqi, M.; Schwarz, H. *Chem. Phys. Lett.* **1994**, *221*, 359.

(10) Anicich, V. G. *J. Phys. Chem. Ref. Data* **1993**, *22*, 1469.

(11) Mallard, W. G.; Linstrom, P. J. *NIST Webbook*; *NIST Standard Reference Database Number 69*; National Institute of Standards and Technology: Gaithersburg, MD, 1998 (http://webbook.nist.gov).

(12) Huber, K. P.; Herzberg, G. *Molecular Spectra and Molecular Structure IV. Constants of Diatomic Molecules*; Van Nostrand Reinhold: New York, 1979.

(13) Lambert, J. D. *Vibrational and Rotational Relaxation in Gases*; Clarendon Press: Oxford, UK, 1977.

(14) Hunter, E. P. L.; Lias, S. G. *J. Phys. Chem. Ref. Data* **1998**, *27*, 413.

(15) Bouchoux, G.; Salpin, J. Y.; Leblanc, D. *Int. J. Mass Spectrom. Ion Processes* **1996**, *153*, 37.

(16) Decker, B. K.; Adams, N. G.; Babcock, L. M. *Int. J. Mass Spectrom.* **1999**, *185/186/187*, 727.

(17) Adams, N. G.; Smith, D. In *Techniques for the Study of Ion−Molecule Reactions*; Farrar, J. M., Saunders, W. H., Eds.; Wiley: New York, 1988; p 165.

(18) Yaws, C. L. *Handbook of Viscosity; Library of Physico-Chemical Property Data*; Gulf Publishing Co.: Houston, TX, 1995.

(19) Taylor, M. D.; Bruton, J. *J. Am. Chem. Soc.* **1952**, *74*, 4151.

(20) (a) Adams, N. G.; Smith, D. *Int. J. Mass Spectrom. Ion Phys.* **1976**, *21*, 349. (b) Adams, N. G.; Smith, D. *J. Phys. B* **1976**, *9*, 1439.

(21) (a) Bartlett, R. J. in *Modern Electronic Structure Theory*; Advanced Series in Physical Chemistry Vol. 2; Yarkony, D. R., Ed.; World Scientific: Singapore, 1995; p 1047. (b) Lee, T. J.; Scuseria, G. E. In *Quantum Mechanical Electronic Structure Calculations with Chemical Accuracy*; Langhoff, S. R., Ed.; Kluwer Academic Press: Dordrecht, 1995; p 47. (c) Crawford, T. D.; Schaefer, H. F. In *Reviews in Computational Chemistry*; Lipkowitz, K. B., Boyd, D. B., Eds.; VCH Publishers: New York, 1999; Vol. 14, p 33.

(22) Purvis, G. D.; Bartlett, R. J. *J. Chem. Phys.* **1982**, *76*, 1910.

(23) Raghavachari, K.; Trucks, G. W.; Pople, J. A.; Head-Gordon, M. *Chem. Phys. Lett.* **1989**, *157*, 479.

(24) (a) Dunning, T. H., Jr. *J. Chem. Phys.* **1989**, *90*, 1007. (b) Woon, D. E.; Dunning, T. H., Jr. *J. Chem. Phys.* **1993**, *98*, 1358.

(25) (a) Woon, D. E.; Dunning, T. H., Jr. *J. Chem. Phys.* **1995**, *103*, 4572. (b) Peterson, K.; Dunning, T. H., Jr., to be published.

(26) Gauss, J.; Lauderdale, W. J.; Stanton, J. F.; Watts, J. D.; Bartlett, R. J. *Chem. Phys. Lett.* **1991**, *182*, 207.

(27) Stanton, J. F.; Gauss, J.; Watts, J. D.; Lauderdale, W. J.; Bartlett, R. J. ACES II, 1993. The package also contains modified versions of the MOLECULE Gaussian integral program of J. Almlöf and P. R. Taylor, the ABACUS integral derivative program written by T. U. Helgaker, H. J. Aa. Jensen, P. Jørgensen, and P. R. Taylor, and the PROPS property evaluation integral code of P. R. Taylor.

(28) Chase, M. W. *NIST-JANAF Thermochemical Tables*; *J. Phys. Chem. Ref. Data* 1998.

(29) Norwood, K.; Ng, C. Y. *Chem. Phys. Lett.* **1989**, *156*, 145.

(30) Walters, E. A.; Blais, N. C. *J. Chem. Phys.* **1984**, *80*, 3501.

(31) Curtiss, L. A.; Raghavachari, K.; Trucks, G. W.; Pople, J. A. *J. Chem. Phys.* **1991**, *94*, 7221.

(32) *Gaussian 94 (*Revision C.3*)*; Frisch, M. J.; Trucks, G. W.; Schlegel, H. B.; Gill, P. M. W.; Johnson, B. G.; Robb, M. A.; Cheeseman, J. R.; Keith, T.; Peterson, G. A.; Montgomery, J. A.; Raghavachari, K.; Al-Laham, M. A.; Zakrzewski, V. G.; Ortiz, J. V.; Foresman, J. B.; Cioslowski, J.; Stefanov, B. B.; Nanayakkara, A.; Challacombe, M.; Peng, C. Y.; Ayala, P. Y.; Chen, W.; Wong, M. W.; Andres, J. L.; Replogle, E. S.; Gomperts, R.; Martin, R. L.; Fox, D. J.; Binkley, J. S.; Defrees, D. J.; Baker, J.; Stewart, J. P.; Head-Gordon, M.; Gonzalez, C.; Pople, J. A. Gaussian, Inc.: Pittsburgh, PA, 1995.

(33) King, R. A.; Allen, W. D.; Ma, B.; Schaefer, H. F. *Faraday Discuss.* **1998**, *110*, 23.

(34) Feller, D. *J. Chem. Phys.* **1992**, *96*, 6104.

(35) Halkier, A.; Helgaker, T.; Jørgensen, P.; Klopper, W.; Koch, H.; Olsen, J.; Wilson, A. K. *Chem. Phys. Lett.* **1998**, *286*, 243.

(36) (a) Peterson, K. A.; Woon, D. E.; Dunning, T. H., Jr. *J. Chem. Phys.* **1994**, *100*, 7410. (b) Dixon, D. A.; Feller, D.; Sandrone, G. *J. Phys. Chem. A* **1999**, *103*, 4744.

(37) Grev, R. S.; Janssen, C. L.; Schaefer, H. F. *J. Chem. Phys.* **1991**, *95*, 5128.

(38) Clabo, D. A.; Allen, W. D.; Remington, R. B.; Yamaguchi, Y.; Schaefer, H. F. *Chem. Phys.* **1988**, *123*, 187.

(39) McQuarrie, D. A. *Statistical Thermodynamics*; University Science Books: Mill Valley, CA, 1973.

(40) Ikezoe, Y.; Matsuoka, S.; Takebe, M.; Viggiano, A. *Gas Phase Ion Molecule Reaction Rate Constants Through 1986*; Maruzen Company, Ltd.: Tokyo, 1987.

(41) Su, T.; Chesnavich, W. J. *J. Chem. Phys.* **1982**, *76*, 5183.

(42) The electric dipole polarizabilities and electric dipole moments are taken from ref 16 and: (a) Lide, D. R. *CRC Handbook of Chemistry and Physics*, 78th ed.; CRC Press: Boca Raton, FL, 1997. (b) Dean, J. A. *Lange's Handbook of Chemistry*, 14th ed.; McGraw-Hill: New York, 1992.

(43) Thomas, J. R.; DeLeeuw, B. J.; Vacek, G.; Crawford, T. D.; Yamaguchi, Y.; Schaefer, H. F. *J. Chem. Phys.* **1993**, *99*, 403.

(44) The enthalpies of formation of the various $[2H,S,O]^+$ isomers are estimated from the CCSD(T) results at 298 K available in Tables 9−11. Uncertainties are estimated to be ±1.5 kcal mol^{-1}. $\Delta H_f^\circ{}_{,298}$(*trans*-$HSOH^+$) is taken to be 188.4 ± 1.5 kcal mol^{-1}, i.e., the average of the coupled cluster CBS results using Schemes 1 and 2.

(45) To the precision of the energetics determined in this study, the difference between the standard temperature of 298.15 K and the experimental temperature of 294.5 ± 2.5 K is negligible.

(46) The recombination energies of the cis and the trans forms of $HSOH^+$ differ by only the 1.9 kcal mol^{-1} difference in their enthalpies of formation (see Table 8), since there is only one isomeric form of the neutral HSOH.

(47) That HOS has a lower proton affinity at the O-atom than the proton affinity of C_2H_4 is inferred from ab initio computational results presented in Tables 8 and 10.

(48) Bohme, D. K. In *Interaction Between Ions and Molecules*; Ausloos, P., Ed.; Plenum: New York, 1975; p 489.

(49) It may also be considered that association is not in direct competition with exothermic proton transfer because the two processes occur in different energy regimes. Association, or stabilization, occurs where proton transfer is not energetically favorable; hence at a low pressure the complex would not be stabilized, but instead would revert to the reactants by unimolecular dissociation. Thus, association at higher pressures can be equated to nonreactivity at the lower pressures considered by Bouchoux et al. This is essentially the argument put forth in our previous study (see ref 16); it is clearly a simplification of the physical situation, but one which is justified in light of the theoretical development of the Bouchoux model.

(50) (a) Lias, S. G.; Shold, D. M.; Ausloos, P. *J. Am. Chem. Soc.* **1980**, *102*, 2540. (b) Ausloos, P.; Lias, S. G. *Int. J. Mass Spectrom. Ion Processes* **1984**, *58*, 165.

(51) In our previous study (see ref 16), it was incorrectly stated that removal of the *trans*-2-butene data point does not change the value for GB(HS_2) obtained from the three-parameter Bouchoux-type fit to the data. A small, but not inconsequential, change is observed, as noted in the text.

(52) The given uncertainties are based on the estimated ±2.0 kcal mol^{-1} uncertainty in the gas basicities of the reference bases (see ref 14) and the 95% confidence intervals for the parameters of the Bouchoux-type fits to the thermokinetic data. See ref 16 for more details.

(53) The positive (+) error bar was determined by combining the 1.9 ± 1.5 kcal mol^{-1} difference in energy between the cis and trans isomers of $HSOH^+$ with the ±2.2 kcal mol^{-1} uncertainty in the gas basicity value obtained directly from the thermokinetic fit.

(54) Cheng, B. M.; Eberhard, J.; Chen, W.-C.; Yu, C.-h. *J. Chem. Phys.* **1997**, *107*, 5273.

(55) Note that the ground electronic states of all three species have identical symmetry, $^2A''$, and thus there is no change in electronic entropy.

(56) For calculation of ΔS_p, the simplification based on the change in rotational symmetry number implies the assumption that vibrational and other entropy changes are negligible compared to rotational entropy changes upon protonation. In light of this, note that for HSO the vibrational and rotational contributions to ΔS_p calculated from the full classical partition function are comparable; e.g., for protonation of HSO to form *trans*-$HSOH^+$, $\Delta S_{rot} = 0.71$ cal mol^{-1} K^{-1} and $\Delta S_{vib} = 0.51$ cal mol^{-1} K^{-1}.